Materials Science in Semiconductor Processing 126 (2021) 105663

Contents lists available at ScienceDirect

Materials Science in Semiconductor Processing

journal homepage: http://www.elsevier.com/locate/mssp

Admittance spectroscopy of dopants implanted in silicon and impurity state-induced AC magnetoresistance effect

D.A. Smolyakov [a,*], A.S. Tarasov [a], M.A. Bondarev [a], A.A. Nikolskaya [b], V.K. Vasiliev [b], M. N. Volochaev [a], N.V. Volkov [a]

[a] Kirensky Institute of Physics, Krasnoyarsk Scientific Center, Siberian Branch, Russian Academy of Sciences, 660036, Russia
[b] Lobachevsky State University, Nizhny Novgorod, 603950, Russia

ARTICLE INFO

Keywords:
Semiconductors
Magnetoimpedance
Impurities
Implantation

ABSTRACT

A silicon structure doped with Ga using ion implantation has been investigated by admittance spectroscopy. It has been established that the presence of the Ga impurity, along with the B one, in the silicon structure leads to the appearance of the second peak in the temperature dependence of the real part of the impedance (admittance). Moreover, switching-on a magnetic field parallel to the sample plane shifts the singularities in the temperature curve to the high-temperature region. This results in the manifestation of both the positive and negative magnetoresistance effect upon temperature and magnetic field variation. It has been found by the standard admittance spectroscopy analysis of the impedance data that the energy structure of the investigated sample includes two interfacial energy levels $E_{S1}(0) = 42$ meV and $E_{S2}(0) = 69.4$ meV. As expected, these energies are consistent with the energies of B and Ga dopants. In a magnetic field, these levels increase by 3 meV for B and 2 meV for Ga, which induces the magnetoresistance effect. It has been demonstrated that the interfacial state-induced magnetoresistance effect can be tuned by ion implantation and dopant selection.

1. Introduction

The devices fabricated using silicon technologies have found wide application in modern microelectronics. For instance, Schottky diodes, due to their manufacturability and universality, have become key elements of electronic and optoelectronic instruments. They represent metal-oxide-semiconductor (MOS) structures, which can serve as a basis of metal-semiconductor field-effect (MESFET) and high electron mobility (HEMT) transistors, solar cells, and photodetectors [1–3].

Meanwhile, the MOS technology is complicated by the extremely high density of states at the oxide/semiconductor interface. A poor interface between an oxide film and a silicon substrate leads to strong leakage currents, pronounced frequency dispersion, high defect density, and, as a consequence, deep levels [4]. The interfacial traps, being major contributors to lowering the efficiency of the discussed structures, are crucial for the quality of the entire device containing an oxide layer [5]. Such interfacial state traps are formed by the destruction of the lattice structure periodicity on the surface when processing the latter and forming a dielectric layer, as well as by impurities in a semiconductor [6].

In view of the aforesaid, study of the interfacial and impurity states is interesting for both the fundamental research and application in future microelectronic devices.

In this work, we mainly use impedance spectroscopy (IS) as an effective tool for analyzing the electrical properties of solids, studying the frequency dependence of the impedance in materials [7], and exploring their dielectric properties [8]. The dc electric response and frequency-dependent behavior of materials can be described in terms of the real and imaginary parts of the complex resistance. In addition, the IS technique allows one to examine impurity centers in semiconductors. This technique is based on the measurements of the real part of the complex admittance at the frequencies and temperatures ensuring the rate of carrier emission from traps comparable with the measuring frequency. The technique was proposed, first used for ZnTe, and described in detail in Ref. [9]. This technique is also called thermal admittance spectroscopy (TAS). Variation of the temperature changes the position of the Fermi level E_F within band gap. At a certain temperature, E_F approaches the levels of impurities or defects. At this point, the test signal modulates the Fermi level so that the traps are filled during half the cycle of the sinusoidal test signal and empty during the second half of the

* Corresponding author.
E-mail address: sda88@iph.krasn.ru (D.A. Smolyakov).

https://doi.org/10.1016/j.mssp.2021.105663
Received 12 October 2020; Received in revised form 17 December 2020; Accepted 3 January 2021
Available online 13 January 2021
1369-8001/

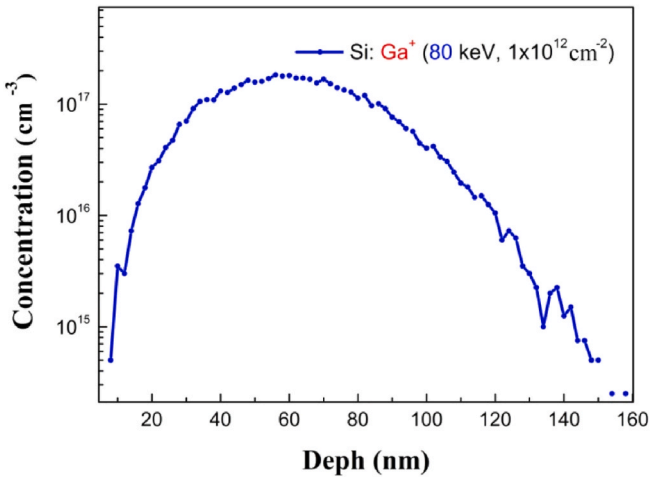

Fig. 1. Distribution of the implanted Ga impurity.

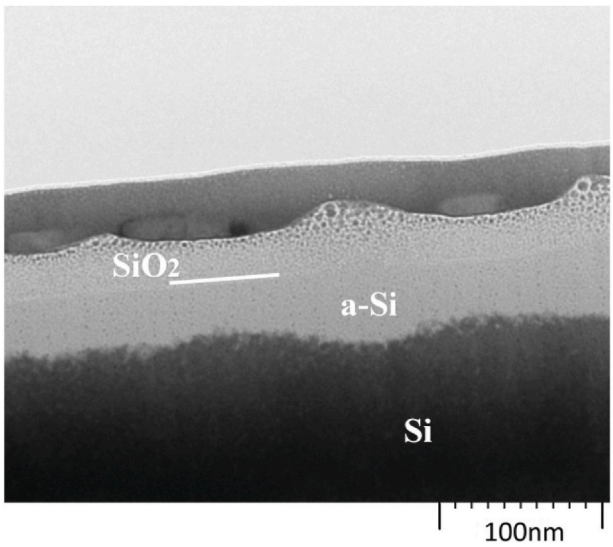

Fig. 2. Transmission Electron Microscopy (TEM) image.

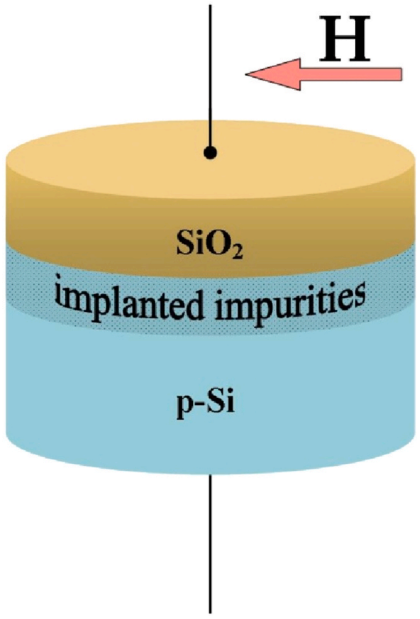

Fig. 3. Schematic of the sample.

cycle. If the natural relaxation frequency is comparable to the signal frequency, then we see a resonance-like increase in the real part of the complex impedance. By measuring impedance versus temperature, characteristic peaks can be observed at specific temperatures, which will depend on frequency.

Earlier, we employed the above-mentioned technique in the investigations and established the magnetoimpedance effect in hybrid structures with a Schottky barrier; the magnetoresistance was found to attain 300% and varied with a dc bias [10]. Further investigations on the silicon-on-insulator (SOI) structures [11] made us thoroughly examine the silicon substrates and impurities in silicon, including implanted ones.

2. Experimental section

The samples were fabricated from single-crystal *p*-Si(100) doped with boron in a concentration of $p = 4 \times 10^{11}$ cm^{-3} and having a resistivity of $\rho = 25$ kΩ. In our previous works, we established that the magnetoimpedance effect was stronger in the samples formed on the *p*-type structures [12]. Moreover, the magnetoimpedance effect is most likely induced by the interfacial levels with the energy similar to that of the boron (phosphorus) levels in silicon. To test this hypothesis, it was proposed to measure the magnetoimpedance in the structures formed on the Si substrates containing other impurities. The most efficient way of introducing desired impurities in a certain concentration to a certain depth is ion implantation. It is used, in particular, in fabricating betavoltaic cells [13], solar cells, transistors, and other semiconductor devices [14].

Along with testing the physical mechanisms responsible for the magnetoimpedance in a nonmagnetic structure, the addition of a dopant or changing its concentration are important for controlling the discussed effect and tuning its value for application in real devices.

The silicon substrate was doped with Ga^+ ions by ion implantation at an energy of $E = 80$ keV in a dose of $\Phi = 1 \times 10^{12}$ cm^{-2}. The depth distributions of ions and ion-induced vacancies are shown in Fig. 1. The calculation was made using the SRIM (Stopping and Range of Ions in Matter) software [15] on an ILU-200 ion-beam facility. Dopant atoms are ionized in an ion source, which can form ion beams of different substances. The ion beam extracted from the source and focused by an electrostatic lens is accelerated by the field of a segment tube and separated by masses with an electromagnetic analyzer.

When interacting with atoms of a target, ions are multiply scattered, lose their energy, and stop at a certain distance from the surface (as a rule, at a depth of 10 nm – 1 μm). Ga atoms was chosen for implantation because the energy of the impurity level formed by them in silicon is sufficiently close to that of boron and phosphorus.

Therefore, there is reason to believe that the magnetoimpedance effect will manifest itself in full degree. The maximum depth of penetration of ions in concentrations above 10^{16} cm^{-3} for Ga is about 100 nm (Fig. 1). After implantation, the impurity concentration and type were changed in the surface region of the Si wafer.

Transmission Electron Microscopy (TEM) study was performed to check the transformation of the sample surface due to gallium irradiation. From cross sectional TEM image (Fig. 2) of implanted sample we can see four layers. From down to top that are monocrystalline silicon (Si), amorphous silicon layer (a-Si), silicon oxide (SiO_2) and tungsten (W) masking layers. Two upper layers were deposited during sample preparation for TEM investigation. As can be seen, a region with a large number of radiation defects (amorphous layer) was formed during Ga implantation. As we have already noted in our previous works [16], such a stratification or layering do not affect measured impedance data due to used experimental technique sense only space charge region of the semiconductor. However, from this figure it is possible to estimate the depth of impurity implantation, which is in good agreement with the

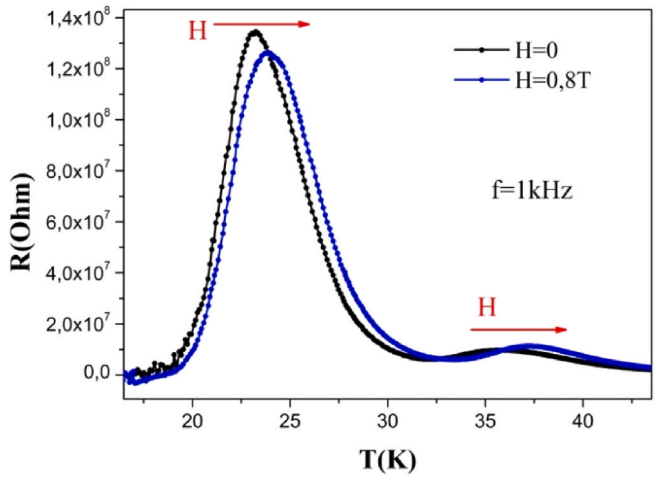

Fig. 4. Temperature dependences $R(T)$ of the real part of the impedance at different frequencies without magnetic field and in a field of 0.8 T.

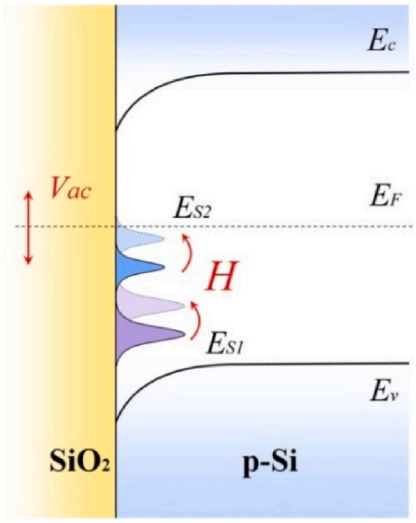

Fig. 5. Schematic band diagram of the sample with the impurity levels. E_F is the Fermi level; E_{S1} and E_{S2} are the B and Ga levels, respectively; and V_{ac} is the applied ac voltage.

SRIM calculations.

The impedance of the structure was measured by a two-probe method. Ohmic contacts were formed using silver epoxy. The contact pad area was 1 mm^2. A schematic of the device is presented in Fig. 3.

The ac investigations were carried out on an Agilent E4980A LCR meter. The ac current frequency ranged from 20 Hz to 2 MHz. An external magnetic field of up to $H = 0.8$ T was applied parallel to the sample plane. The measurements were performed in a helium cryostat in the temperature range of 4.2–350 K.

3. Results and discussion

The examination of the transport properties of the samples was started with the temperature dependences $R(T)$ of the real part of the impedance $Z = R + iX$. Below 50 K, the singularities (peaks) were observed (Fig. 4). These singularities are well-known in admittance spectroscopy, which is based on the measurements of the real part of the complex admittance at frequencies and temperatures ensuring the rate of carrier emission from traps comparable with the measuring frequency [17].

These $R(T)$ peaks appear due to the presence of impurity centers and

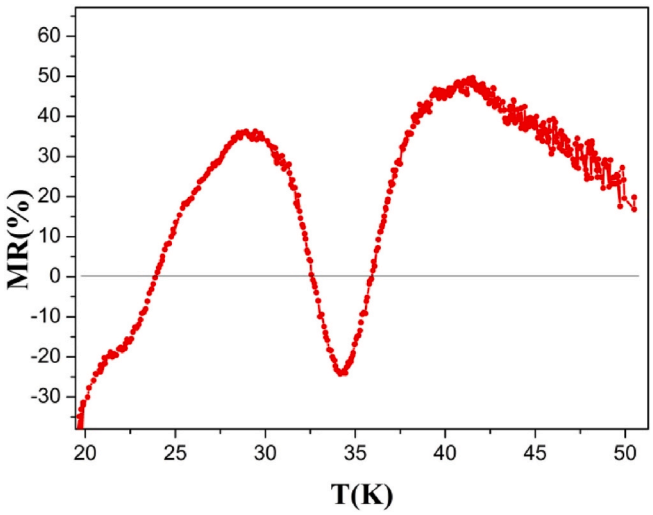

Fig. 6. Temperature dependence of the magnetoresistance in a magnetic field of 0.8 T.

their participation in the carrier emission/capture processes. At a certain temperature, when Fermi level E_F starts crossing energy levels E_S of the surface states, ac bias V_{ac} across the MIS structure modulates the position of E_S relative to E_F, thereby initiating the capture/emission of electrons from the interfacial states to the valence band (Fig. 5).

The peak in the $R(T)$ dependence should occur under the condition $\omega\langle\tau_0\rangle = 1$, where $\omega = 2\pi f$ is the angular frequency of V_{ac} and $\langle\tau_0\rangle$ is the average relaxation time, which characterizes the interfacial state charging-discharging process.

These features were observed by us in the MIS structures [16]. However, in the previous works, we observed the only the peak typical of the phosphorous or boron impurity, depending on a chosen Si substrate type. Here, we have two such peaks. The second peak appeared in the region of higher temperatures and has a smaller amplitude. This speaks about the occurrence of another impurity level. A decrease in the peak amplitude can be caused by the broader energy distribution of impurities during implantation than at the crystal growth of doped silicon. As a result, at a certain temperature, the smaller amount of impurities is involved in the emission/capture of carriers.

In external magnetic field H, the $R(T)$ singularities shift by 2 K toward higher temperatures. Due to the presence of two singularities, we can observe the magnetoresistance $MR = 100*((R(H)–R(0))/R(0))$ at two temperatures simultaneously (Fig. 6).

This effect of the magnetic field is related to the shift of the energy levels of the impurity states toward higher energies (toward the semiconductor band gap center). This provides prospects for use of impurities with different energies for obtaining a singularity and, consequently, the magnetoresistance, at specified temperatures. This approach offers the opportunity for finer tuning and using the magnetoresistance effect. We cannot describe the exact nature of this phenomenon within the framework of this work. Nevertheless, the shift of the energy levels of the impurity centers in magnetic field towards higher energies is typical to doped semiconductors. This effect was observed, for example, in p-doped Si [18] and n–-type GaAs [19]. Two possible models were discussed: (1) shrinkage of the impurity center wave functions caused by magnetic field; (2) splitting of the impurity band into lower and higher subbands. However, in neither case, specific microscopic mechanisms of the change in the electronic structure of the impurity centers in a magnetic field were clarified in zero magnetic field ($E_S(0)$) and in a field of 0.8 T ($E_S(H)$).

Then, we estimated the energy of the impurity states in zero and nonzero magnetic fields using the relation $ln(\omega) = ln(1/\tau_0) - E_s/(k_B T_p)$ [20], where T_p is the $R(T)$ peak position at constant ω, τ_0 is the average

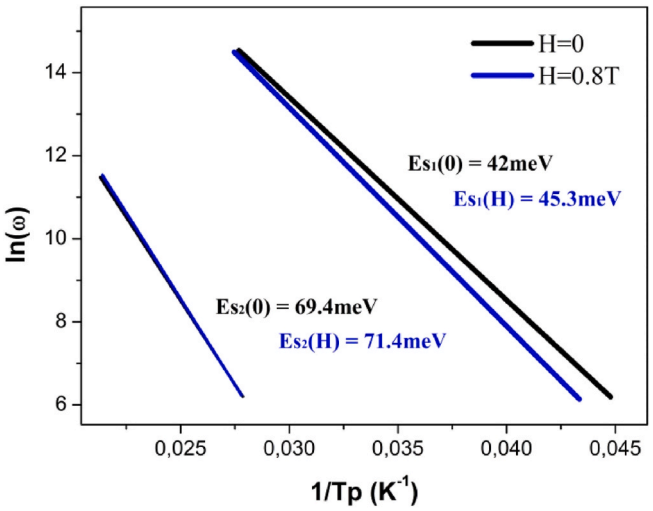

Fig. 7. ln(ω) vs reciprocal peak temperature 1/Tp for determining the energy levels of the impurities states.

relaxation time, and k_B is the Boltzmann constant. The energy was estimated by linear fitting of the experimental dependence of $ln(\omega)$ on $1/T_p$ from the slope of the fitting line (Fig. 7).

It can be seen that, for the lower-temperature peak, the energy of the impurity centers is $E_{S1}(0) = 42$ meV without magnetic field and $E_{S1}(H) = 45.3$ meV in a field of $H = 0.8$ T. The obtained energy agrees well with the energy of the boron impurity for the *p*-type substrate. The energy of the impurity states of the second peak located in the higher-temperature region are different: $E_{S2}(0) = 69.4$ meV and $E_{S2}(H) = 71.4$ meV. Addressing to the energies of impurities in semiconductors [21], we can see that the obtained second-peak energy is close to the gallium energy.

Thus, the impedance spectroscopy investigations revealed the presence of energy levels not only for the conventional boron impurity, but also for the implanted gallium dopant. Despite the fact that the implanted layer strongly damaged this is insignificant due to measurement technique used.

4. Conclusions

In this study, we investigated the transport and magnetotransport properties of the semiconductor implanted with the Ga dopant. Below 50 K, the peak singularities were observed. In contrast to the previous works, where the observation of the only peak was reported, here we had two such peaks. This allowed us to state the occurrence of another impurity level. Under the action of a magnetic field, the singularities shift toward higher temperatures and the maximum magnetoresistance at two temperatures simultaneously was observed. The energies of the impurity states in zero and nonzero magnetic fields were calculated. It was found that, for the peak at 20 K, the obtained energy corresponds to the boron dopant energy for the *p*-type substrate and the energies of the second peak are consistent with the energy of implanted Ga. Thus, the assumptions based on the previous studies were confirmed. This allowed us to conclude that, during implantation of some impurities, the magnetoresistance can be obtained at certain temperatures. The bandgap engineering and ion implantation techniques offer the opportunities for use of the examined effect in the development of electronic devices exploiting the magnetoresistance and magnetoimpedance effects.

Author statement

D. A. Smolyakov: Investigation, Formal analysis, Writing - Original Draft.
A. S. Tarasov: Writing - Review & Editing, Project administration.
M. A. Bondarev: Visualization.
A. A. Nikolskaya: Resources.
V.K. Vasiliev: Validation.
M. N. Volochaev: Transmission Electron Microscopy.
N. V. Volkov: Methodology, Conceptualization, Supervision.

Declaration of competing interest

The authors declare that they have no known competing financial interests or personal relationships that could have appeared to influence the work reported in this paper.

Acknowledgements

This study was supported by the Government of the Russian Federation, Mega Grant for the Creation of Competitive World-Class Laboratories (Agreement no. 075-15-2019-1886).

The authors thank the Krasnoyarsk Territorial Shared Resource Center, Krasnoyarsk Scientific Center, Russian Academy of Sciences, for allowing our electron microscope investigations.

References

[1] S. Alptekin, A. Tataroğlu, Ş. Altındal, J. Mater. Sci. Mater. Electron. 30 (2019) 6853–6859.
[2] H.G. Çetinkaya, M. Yıldırım, P. Durmuş, Ş. Altındal, A.C. Sc, J. Alloys Compd. 728 (2017) 896–901.
[3] D.E. Yildiz, Ş. Altindal, H. Kanbur, J. Appl. Phys. 103 (2008) 124502.
[4] T. Hori, Springer Series in Electronics and Photonics, vol. 34, 1997.
[5] P. Hanselaer, W.H. Laflere, R.L. Van Meirhaeghe, F. Cardon, J. Appl. Phys. 56 (1984) 2309–2314.
[6] E.H. Nicollian, A. Goetzberger, Appl. Phys. Lett. 7 (1965) 216–219.
[7] E. Barsoukov, J.R. Macdonald, Impedance Spectroscopy Theory, Experiment, and Applications, second ed., 2005.
[8] V.F. Lvovich, Impedance Spectroscopy: Applications to Electrochemical and Dielectric Phenomena, 2012.
[9] J.L. Pautrat, B. Katircioglu, N. Magnea, D. Bensahej, J.C. Pfistert, L. Revoil, Solid State Electron. 23 (1980) 1159.
[10] N.V. Volkov, A.S. Tarasov, D.A. Smolyakov, S.N. Varnakov, S.G. Ovchinnikov, JMMM 383 (2015) 69–72.
[11] D.A. Smolyakov, A.S. Tarasov, I.A. Yakovlev, M.N. Volochaev, Semiconductors 53 (14) (2019) 1964–1966.
[12] D.A. Smolyakov, A.S. Tarasov, I.A. Yakovlev, A.N. Masyugin, M.N. Volochaev, I. A. Bondarev, N.N. Kosyrev, N.V. Volkov, Thin Solid Films 671 (2019) 18–21.
[13] A. Krasnov, S. Legoti, K. Kuzmina, N. Ershova, B. Rogozev, Nuclear Engineering and Technology 51 (8) (2019) 1978.
[14] I. Michael, Industrial Accelerators and Their Applications, 2012, pp. 57–85.
[15] J.F. Ziegler, M.D. Ziegler, J.P. Biersack, Nucl. Instrum. Methods Phys. Res., Sect. B 268 (2010) 1818–1823.
[16] N.V. Volkov, A.S. Tarasov, D.A. Smolyakov, A.O. Gustaitsev, M.V. Rautskii, A. V. Lukyanenko, M.N. Volochaev, S.N. Varnakov, I.A. Yakovlev, S.G. Ovchinnikov, AIP Adv. 7 (2017), 015206.
[17] A.R. Peaker, V.P. Markevich, J. Coutinho, J. Appl. Phys. 123 (2018) 161559.
[18] J.J.H.M. Schoonus, F.L. Bloom, W. Wagemans, H.J.M. Swagten, B. Koopmans, Phys. Rev. Lett. 100 (2008) 127202.
[19] T.W. Hickmott, Phys. Rev. B 46 (1992) 12324.
[20] D.L. Losee, J. Appl. Phys. 46 (1975) 2204.
[21] S.M. Sze, Kwok K. Ng, Physics of Semiconductor Devices, 2007.